Hunting η-bound nuclei

H. Machner[1,2;1)]

[1] Institut für Kernphysik, Forschungszentrum Jülich, 52428 Jülich, Germany
[2] Fakultät für Physik, Universität Duisburg-Essen, Lotharstr. 1, 47048 Duisburg

Abstract The η meson can be bound to atomic nuclei. Experimental search is discussed in the form of final state interaction for the reactions $dp \to {}^3He\eta$ and $dd \to {}^4He\eta$. For the latter case tensor polarized deuterons were used in order to extract the s-wave strength. For both reactions complex scattering lengths are deduced: $a_{^3He\eta} = \left[\pm\left(10.7\pm0.8^{+0.1}_{-0.5}\right)+i\cdot\left(1.5\pm2.6^{+1.0}_{-0.9}\right)\right]$ fm and $a_{^4He\eta} = [\pm(3.1\pm0.5)+i\cdot(0\pm0.5)]$ fm. In a two-nucleon transfer reaction under quasi-free conditions, $p{}^{27}Al \to {}^3HeX$, was investigated. The system X can be the bound $^{25}Mg\otimes\eta$ at rest. When a possible decay of an intermediate $N^*(1535)$ is required, a highly significant bump shows up in the missing mass spectrum. The data give for a bound state a binding energy of 13.3±1.6 MeV and a width of σ=4.4±1.3 MeV.

Key words η meson production, η nucleus interaction, final state interaction, recoil free kinematics

PACS 21.85.+d, 13.75.-n

1 Introduction

In contrast to the pion-nucleon interaction, the η-nucleon interaction at small momenta is attractive and rather strong. This attraction can be seen from the fact that the η threshold (1488 MeV) is situated just below the $N^*(1535)$ resonance which couples strongly to the η−N channel. Initial calculations by Bhalerao and Liu [1] obtained attractive s-wave $\eta - N$ scattering lengths. With these values, Haider and Liu [2] have shown that η can be bound in nuclei with A ⩾ 10. Other groups have also found similar results [3–5].

On the experimental side results are meager. The first experiments searching for η-mesic nuclei at BNL [6] and LAMPF [7] by using a missing-mass technique in the (π^+,p) reaction reached negative or inconclusive results. Later it became clear that the peaks are not necessarily narrow and that a better strategy of searching for η-nuclei is required. Furthermore, the BNL experiment was in a region far from the recoilless kinematics, so that the cross section is substantially reduced [8]. More recently, the existence of η-mesic ^{3}He was claimed to have been observed in the reaction $\gamma{}^3He \to \pi^0 pX$ using the photon beam at MAMI [9]. It has, however, been pointed out [10] that the data of Ref. [9] does not permit an unambiguous determination of the existence of a ^{3}Heη-bound state. The suggestion that ^{3}Heη is not bound is also supported by the theoretical studies of Refs. [11, 12].

Two different methods have been applied in the search for η bound states. One is the study of η production on nuclei and extraction of the η nucleus scattering length. The other is the direct production of the η meson in a bound state. This state is measured via missing mass technique. The GEM collaboration [13] has used both methods, as will be shown in this paper.

2 Searches via final state interaction

According to the Watson-Migdal theory [14, 15], when there is a weak transition to a system where there is a strong final state interaction (FSI), one can factorize the s-wave reaction amplitude, f_s, near threshold in the form

$$f_s = \frac{f_B}{1 - iap_\eta}, \tag{1}$$

where p_η is the η c.m. momentum and A the complex scattering length. The unperturbed production

Received 19 January 2010

1) E-mail: h.machner@fz-juelich.de

amplitude f_B is assumed to be slowly varying and is often taken to be constant in the near-threshold region.

Unitarity demands that the imaginary part of the scattering length be positive, i.e., $a_i > 0$. In addition, to have binding, there must be a pole in the negative energy half-plane, which requires that [11]

$$|a_i|/|a_r| < 1\,. \tag{2}$$

Finally, in order that the pole lie on the bound- rather than the virtual-state plane, one needs also $a_r < 0$.

Recently, two different experiments at COSY Jülich measured η production in pd → η^{3}He reactions very close to threshold with an extremely high precision of the data [16, 17].

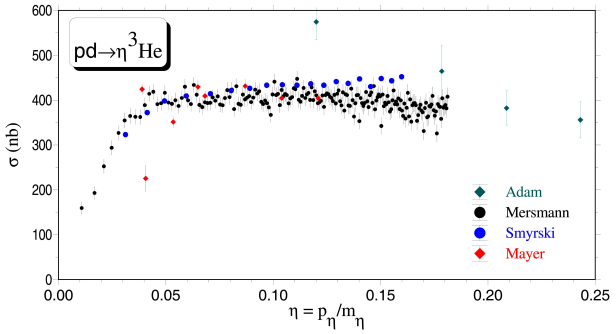

Fig. 1. (color online) Excitation function for the reaction pd → η^{3}He in the threshold region as function of the dimensionless η momentum $\eta = p_\eta/m_\eta$.

In Fig. 1 we compare these new data with others from Refs. [16–19] in the threshold region. The width of the beam is not folded out. However, in the final analysis Mersmann et al. [16] did this, which is crucial for data close to the threshold. The rapid rise of the cross section close to the threshold is a clear indication of a strong final state interaction. Whereas Smyrski et al. [17] claimed that only a scattering length is sufficient to describe the data, Mersmann et al. [16] found a better description when an effective range is also taken into account. The result of the first group is

$$a_{^3\mathrm{He}\eta} = [\pm(2.9\pm2.7) + i\cdot(3.2\pm1.8)]\ \text{fm}, \tag{3}$$

while the second group reported

$$a_{^3\mathrm{He}\eta} = \left[\pm\left(10.7\pm0.8^{+0.1}_{-0.5}\right) + i\cdot\left(1.5\pm2.6^{+1.0}_{-0.9}\right)\right]\ \text{fm} \tag{4}$$

and

$$r_0 = \left[(1.9\pm0.1) + i\cdot\left(2.1\pm0.2^{+0.2}_{-0.0}\right)\right]\ \text{fm} \tag{5}$$

for the effective range. Since the data are not sensitive to the sign of the real part of the scattering length, the quest for a bound state or an unbound pole can not be answered. Its value is

$$|Q_{^3\mathrm{He}\eta}| \approx 0.30\ \text{MeV}. \tag{6}$$

From the model calculations it is known that binding is more probable for heavier nuclei than for lighter nuclei. We therefore can expect the relation

$$|Q_{^3\mathrm{He}\eta}| < |Q_{^4\mathrm{He}\eta}| \tag{7}$$

to hold. In the following we study of the FSI of the η ^{4}He system. This is produced in the reaction

$$\mathrm{dd} \to \eta\alpha\,. \tag{8}$$

The existing data before the GEM measurement were not sufficient to extract the s-wave contribution of the cross section. In order to do so GEM made use of a tensor polarized deuteron beam [20]. The beam momentum of 2385.5 MeV/c corresponds to an excess energy of $Q = 16.6$ MeV for this reaction when an η-meson mass of $m_\eta = 547.7$ MeV/c^2 is used [21]. The Big Karl magnetic spectrograph [22, 23] employed for this study is equipped with two sets of multi-wire drift chambers (MWDC) for position measurement and thus track reconstruction. Two layers of scintillating hodoscopes, 4.5 m apart, led to a more accurate time-of-flight measurement than previously achieved with Big Karl. They also provided the energy-loss information necessary for particle identification. More information on the experiment are given in Ref. [20].

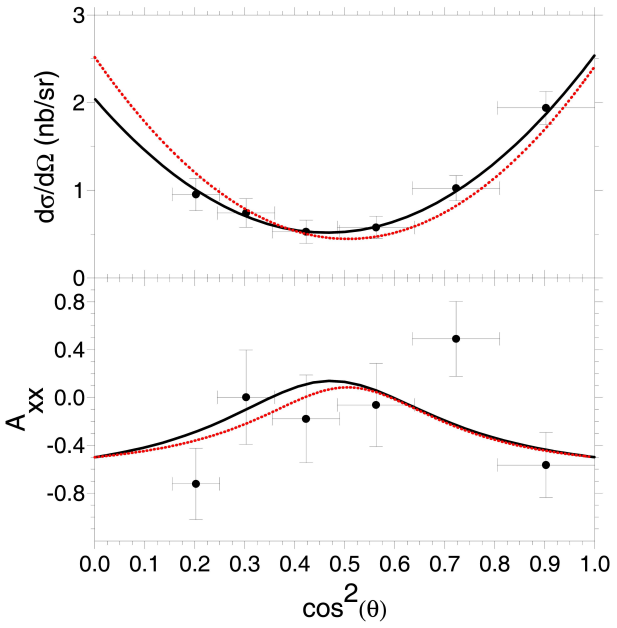

Fig. 2. (color online) Upper panel: Differential cross section for the dd → αη reaction. Lower panel: Analyzing power A_{xx}. The solid curves represent a fit with four partial waves; the dotted curves with invariant amplitudes.

In a first step the unpolarized cross section was measured.

The obtained angular distribution is shown in Fig. 2. It can be fitted by Legendre polynomials. Because of the symmetric entrance channel only even polynomials contribute. Three parameters are sufficient to reproduce the data. This indicates that there must be at least d-wave contributions. This is to be contrasted to the lower energy ANKE results [24], where $2\ell_{\max}=2$ suffices. From the fit total cross section of $\sigma=16.0\pm0.4$ nb, where uncertainties in the target thickness, incident flux, and acceptance introduce an additional systematic error of ±1.6 nb.

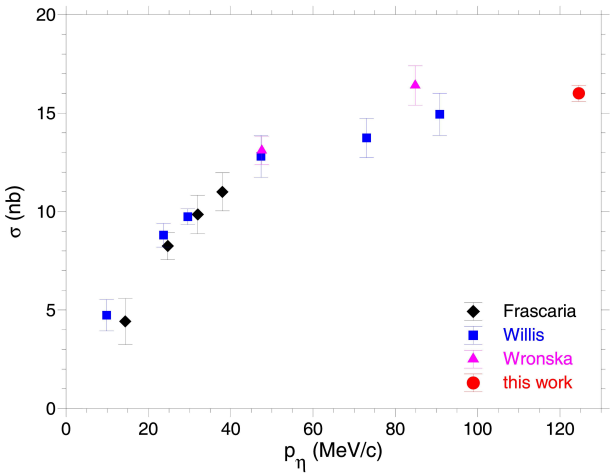

Fig. 3. (color online) Excitation function for the total cross section for the dd $\to \alpha\eta$ reaction. Only statistical errors are shown.

This value is shown in Fig. 3 together with the world data [24–26]. It seems that the cross sections start to saturate for η momenta above 80 MeV/c.

The next step is to extract the s-wave part of the total cross section. For this task the knowledge of polarization observables is necessary. First the polarization of the beam p_{zz} was measured by measuring elastic backward scattering of the deuterons on protons. From the known analyzing power A_{yy} the beam polarization is obtained. In the measurement of analyzing powers one usually compares polarized and unpolarized cross sections. This introduces ambiguities because of different luminosity measurements. In order to avoid this we applied another method. We integrated the cross section over intervals in the polar angle, where on one hand we have full geometrical acceptance of the apparatus and A_{yy} practically vanishes. We measure then only A_{xx}. the cross section integrated over these intervals of azimuthal angle becomes simply

$$I=\int_{(\pi-1)/2}^{(\pi+1)/2}\left(\frac{\mathrm{d}(\theta,\phi)}{\mathrm{d}\Omega}\right)_{\mathrm{pol}}\mathrm{d}\phi= \left(\frac{\mathrm{d}\sigma}{\mathrm{d}\Omega}(\theta)\right)_{\mathrm{unpol}}[1+0.46\,p_{zz}A_{xx}(\theta)]\,, \tag{9}$$

where the unpolarized cross section is integrated over the same ϕ range.

Carrying out this procedure for the two polarization states, we find that

$$\Delta=\frac{I^+-I_1^-}{I^++I^-}=\frac{0.23\,A_{xx}\,(p_{zz}^+-p_{zz}^-)}{1+0.23\,A_{xx}\,(p_{zz}^++p_{zz}^-)}\ . \tag{10}$$

and hence

$$A_{xx}=02.44\Delta\ . \tag{11}$$

The angular distribution thus obtained is also shown in Fig. 2. From both angular distributions we extract partial waves, one s-wave, one p-wave and two d-waves. This yields seven parameters to be fitted. However, strong correlations were found. An alternative method is to employ the spin structure of the matrix element. Due to the symmetry in the entrance channel three independent scalar amplitudes are necessary to describe the spin dependence of the reaction: A, B, C. B and C have no angular dependence and for A we assume the expansion $A=A_0+A_2P_2(\cos\theta)$. Fortunately the dependencies can be decoupled

$$(1-A_{xx})\frac{\mathrm{d}\sigma}{\mathrm{d}\Omega}=\frac{p_\eta}{p_\mathrm{d}}\big(|A_0|^2+2\mathrm{Re}(A_0A_2^*)P_2(\cos\theta)+ |A_2|^2\,(P_2(\cos\theta))^2\big), \tag{12}$$

$$(1+2A_{xx})\frac{\mathrm{d}\sigma}{\mathrm{d}\Omega}=2\frac{p_\eta}{p_\mathrm{d}}\big(|B|^2\sin^2\theta\cos^2\theta+|C|^2\sin^2\theta\big). \tag{13}$$

We now extract the magnitude of the s-wave amplitude $|a_0|$. From this we obtain a spin-averaged square of the s-wave amplitude, $|f_s|^2$ through

$$\frac{\mathrm{d}\sigma_s}{\mathrm{d}\Omega}=\frac{p_\eta}{p_\mathrm{d}}|f_s|^2=\frac{2p_\eta}{3p_\mathrm{d}}|A_0|^2=\frac{1}{27}\frac{1}{4\pi}|a_0|^2\ . \tag{14}$$

Wrońska et al. [24] could not distinguish whether the angular distribution is due to a $s-p$ interference or a d-wave. This puzzle can be solved by our result here. The Willis et al. [26] data for s-wave were extracted from the measurement by just dividing by 4π. This is, however, not justified in the region of their highest point. Assuming a dependence of the d-waves with p_η^2 we can extract a more correct value for the s-wave strength. From all measurements we then obtain a scattering length of

$$a_{^4\mathrm{He}\eta}=[\pm(3.1\pm0.5)+i\cdot(0\pm0.5)]\ \mathrm{fm}. \tag{15}$$

This result can be converted into a pole position

$$|Q_{^4\mathrm{He}\eta}| \approx 4 \text{ MeV}. \quad (16)$$

Since the present results fulfill the conditions for a bound state - except for the sign of the real part of the scattering length - and the relation 7, it may well be that $\eta - \alpha$ binding is observed.

3 Production of η bound nuclear states

The following method was successfully employed in the production of Hypernuclei and pionic atoms. A nucleon is replaced by a hyperon or a pion. Maximal cross section is obtained when the momentum transfer from the projectile to the particle to be implanted is minimized, which means that the produced particle is almost at rest in the laboratory system. In pionic atom studies a proton transfer via the (d, ^{3}He) reaction was successfully applied [27]. However, although this reaction has reasonably large cross section it also has the disadvantage of a huge background due to the break-up of the deuterons. The resulting protons have the beam velocity and thus the same magnetic rigidity as the ^{3}He particles. This problem can be overcome by making use of a two-nucleon transfer reaction like (p, ^{3}He) but at the expense of a much smaller cross section. The choice of an odd-odd target nucleus would be ideal in order to avoid nuclear excitations as much as possible. Since there exist no solid material with these properties ^{27}Al was chosen as a compromise. The experiment was done by making use of the following reaction chain:

$$\mathrm{p} + {}^{27}\mathrm{Al} \rightarrow {}^3\mathrm{He} + \mathrm{X} \quad (17)$$

where the ^{3}He carries the beam momentum away. The unobserved system X is therefore at rest. One of the possibilities is $\mathrm{X} = {}^{25}\mathrm{Mg} + \eta$. Since the η is also at rest it can undergo a second chain of reactions

$$\eta + \mathrm{N} \leftrightarrows \mathrm{N}^* \rightarrow \mathrm{N}\pi. \quad (18)$$

The final fate of that chain is the decay to a pion and a nucleon. In the case of a neutral resonance the final state can be $\mathrm{p} + \pi^-$, which have to be emitted almost back to back, if we ignore Fermi motion. The ^{3}He is detected with the magnetic spectrograph Big Karl [22, 23]. For the detection of the two decay particles a dedicated detector ENSTAR was built. It has cylindrical shape around the target and consists of three layers of scintillating material. The layers were subdivided into pieces making polar and azimuthal angle measurements possible. The read-out of the pieces was performed with scintillating fibres [28]. The detector is shown during its assembling phase in Fig. 4.

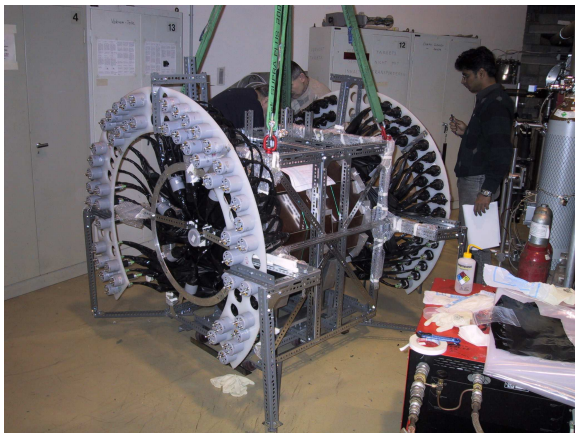

Fig. 4. (color online) The ENSTAR detector during assembling.

The experiment was performed at a beam momentum of 1745 MeV/c. At this momentum final states with small binding energies can be produced with small momentum transfer. States with binding energies from 0 MeV to −30 MeV will have momenta below 30 MeV/c.

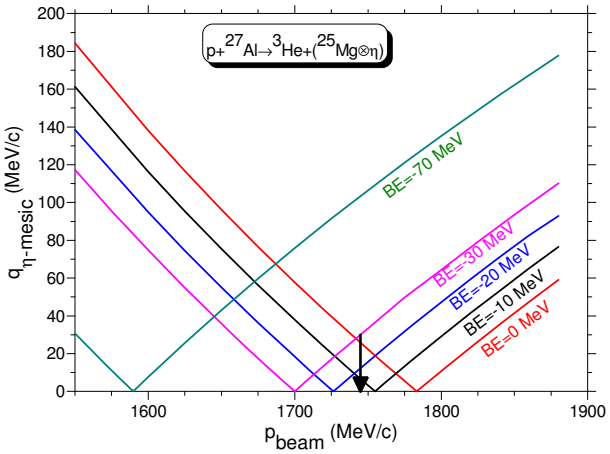

Fig. 5. (color online) Momentum transfer to the η mesic system as function of the beam momentum for the deuteron transfer reaction. The curves show the relation for different binding energies. The arrow shows the presently used beam momentum.

Two settings of the spectrograph were used with a large overlap. Excellent particle identification in Big Karl was achieved by measuring energy loss in the start detector of the TOF facility in the focal plane and TOF.

In the upper panel of Fig. 6 the time of flight is shown without any constraint. The different bumps

are due to different revolutions in the synchrotron. The needles on the third bump are from different particle species: ^{3}He, ^{3}H and ^{4}He. In the middle panel ^{3}He are selected. The lower panel shows the spectrum when a coincidence with the ENSTAR detector is required in addition. The mean of the areas marked L(eft) and R(ight) are subtracted finally as background.

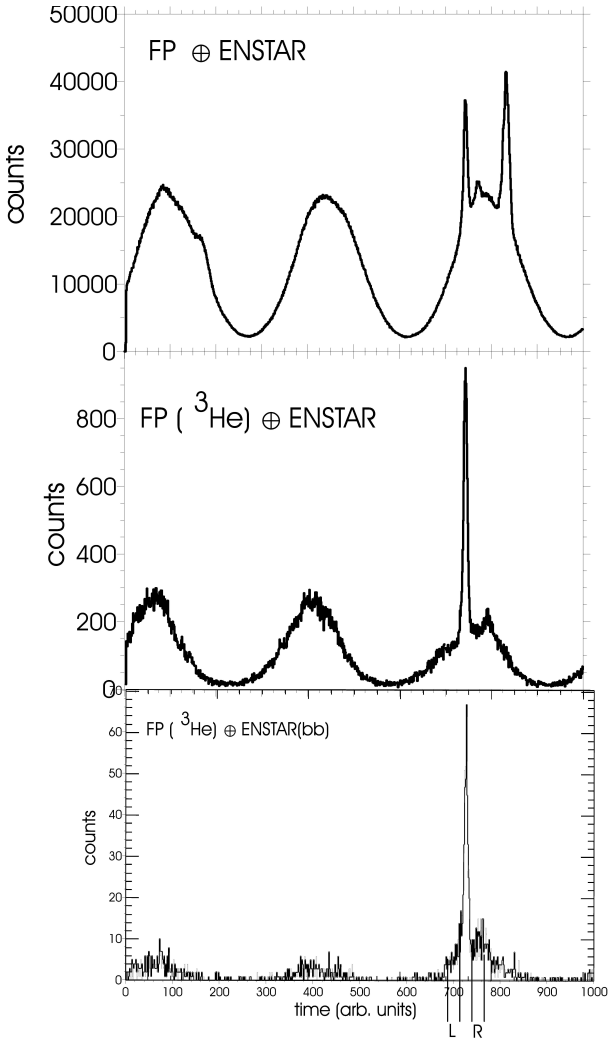

Fig. 6. (color online) The measured time-of-flight (TOF) in the focal plane of Big Karl under different boundary conditions indicated next to the appropriate spectrum.

In test runs the detector elements of ENSTAR were calibrated with cosmics and reaction products from two-body reactions. It was found to be sufficient to require, in addition of the angle measurement, one particle being stopped in the middle layer, i.e. the proton and the second to punch through all three layers, i.e. the pion. Such a situation is sketched in Fig. 7.

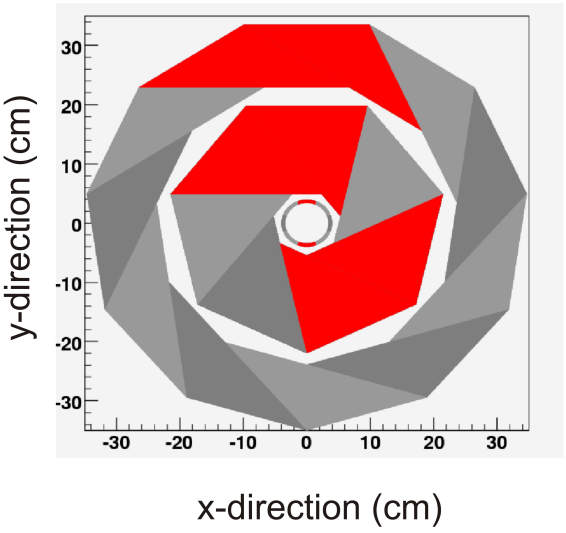

Fig. 7. (color online) Cross section of the ENSTAR detector. Scintillating pieces fired during a decay $N^* \to p + \pi^-$ are shown in red.

Figure 8 shows the measured missing mass spectra. The most upper curve represents Eq. (17). Here X can be any system excited to ≈550 MeV, but with no linear momentum. Therefore only the requirement of a back-to-back emission of two particles is not sufficient to identify step Eq. (18). The unconstrained data do not show any structure and can be well described by a constant. For the data in the lowest spectrum, the N^* decay pattern is required. The counts are typically lower by three orders of magnitude than those in the unconstrained case and an order of magnitude compared to the case without the back-to-back requirement. Although, the $N^*(1535)$ can also decay with two-pion emission, this branch is small compared to the $p\pi^-$ channel.

The data show an enhancement around $BE \approx -13$ MeV. The significance of this structure is extracted according to the two methods given in Refs. [29] and [30] respectively. At first, we test the hypothesis of peak structure being a fluctuation of background, i.e. the origin of the background is taken to be independent of the signal. The background outside the peak region, for simplicity approximated by a constant, was found to be 5.8±0.64. The significance [29] is then given by $(N - BG)/\sqrt{BG + \sigma_{BG}}$ where N is the total counts in the region of interest, BG is the total background in this region as determined from the fit to the outside region and σ_{BG} is error in the estimation of background value as taken from the fit. This yields a value of significance which is 5.3σ. Here we have assumed Gaussian errors. For the assumption of Poisson errors with asymmetric error bars (see Fig. 8) the background is 6.2±1.0.

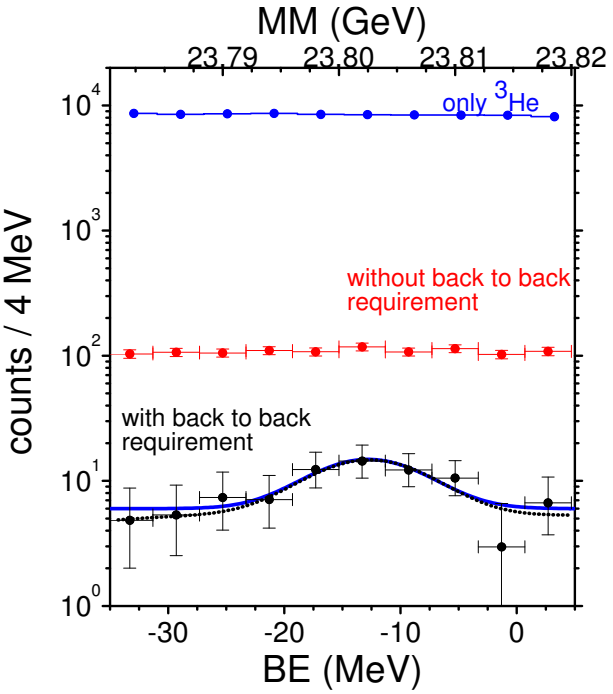

Fig. 8. (color online) Missing mass spectra as measured with the magnetic spectrograph. The upper abscissa is the missing mass while the lower is the binding energy of a bound system ^{25}Mg⊗η (see text).

This larger value is typical for Poisson distribution and hence the significance reduces to 4.9σ. Finally a Gaussian on top of the background was fitted to the whole data set. This yielded for the case of Poisson statistics 6.4±0.96 for the background, 8.3±3.6 for the amplitude, −12.0±2.2 MeV for the centroid and 4.7±1.7 MeV for the width. The corresponding curves are shown in Fig. 8. In the second method, the statistical significance is extracted by assuming the background events as well as the peak events on top of the background being Poisson distributed. Again a constant background and a Gaussian was assumed. A fit was performed using the maximum likelihood method. The significance is then defined as, $\sqrt{-2\Delta lnL}$. Here, ΔlnL is the difference in the values of the logarithm likelihood function with signal fixed to zero and at the best fit value. In this way, we obtain a value of 6.20σ for the significance, assuming a simultaneous determination of amplitude, centroid and width of the signal. The fit gives for the linear background 6.38 ± 0.53 together with the values, for the signal amplitude 8.55 ± 3.05, for the centroid −13.13±1.64 MeV and for the width 4.35±1.27 MeV corresponding to a FWHM of 10.22±2.98 MeV. These results compare favorably with those from the first method. We, therefore, consider the present experimental results to provide a strong hint of a nuclear η bound state.

This allows us to give an upper bound for the cross section. With an estimated efficiency due to detector geometry and analysis selections of 0.70±0.07 we find σ = 0.152±0.054 (stat) ±0.021 (syst) nb. If this "structure" corresponds to a bound η decaying via reaction (Eqn. 18), the cross section would be 0.46±0.16 (stat) ±0.06 (syst) nb, assuming an isospin branching ratio of 1/3.

The author is grateful to the members of the GEM collaboration. Discussions with C. Wilkin have been helpful.

References

1 Bhalerao R S, LIU L C. Phys. Rev. Lett., 1985, **54**: 865
2 Haider Q, LIU L C. Phys. Lett. B, 1986, **172**: 257
3 Garcia-Recio C, Inoue T, Nieves J, Oset E. Phys. Lett. B, 2002, **550**: 47
4 Hayano R S, Hirenzaki S, Gillitzer A. Eur. Phys. J. A, 1999, **6**: 99
5 Tsushima K. Nucl. Phys. A, 2000, **670**: 198c
6 Chrien R E et al. Phys. Rev. Lett., 1988, **60**: 2595
7 Lieb J B. Proc. International Conf. Nuclear Physics, Sao Paulo, Sao Paulo, Brazil, 1988
8 Nagahiro H, Jido D, Hirenzaki S. Phys. Rev. C, 2009, **80**: 025205
9 Pfeiffer M et al. Phys. Rev. Lett., 2004, **92**: 252001
10 Hanhart C. Phys. Rev. Lett., 2005, **94**: 049101
11 Haider Q, LIU L C. Phys. Rev. C, 2002, **66**: 045208
12 Sofianos S A, Rakityansky S A. arXiv, 1997, **nucl-th**: 9707044
13 www.fz juelich.de/ikp/gem/
14 Migdal A B. JETP, 1955, **1**: 2
15 Watson K M. Phys. Rev., 1952, **88**: 1163
16 Mersmann T et al. Phys. Rev. Lett., 2007, **98**: 242301
17 Smyrski J et al. Phys. Lett. B, 2007, **649**: 258
18 Adam H H et al. Phys. Rev. C, 2007, **75**: 014004
19 Mayer B et al. Phys. Rev. C, 1996, **53**: 2068
20 Budzanowski A et al (The GEM collaboration). Nucl. Phys. A, 2009, **821**: 193
21 Hagiwara K et al (PDG). Phys. Rev. D, 2002, **66**: 010001
22 Bojowald H et al. Nucl. Instruments and Meth. in Phys. Res. A, 2002, **487**: 314
23 Drochner M et al. Nucl. Phys. A, 1998, **643**: 55
24 Wrońska A et al. The European Physical Journal A, 2005, **26**: 421
25 Frascaria R et al. Phys. Rev. C, 1994, **50**: R537
26 Willis N et al. Phys. Lett. B, 1997, **406**: 14
27 Ymazaki T et al. Z. Physik A, 1996, **355** 219
28 Betigeri M et al. Nucl. Instruments and Meth. in Phys. Res. A, 2007, **578**: 198
29 Frodesen A G, Skjeggstad O, Töfte H. Probability and Statistics in Particle Physics, Universitetsforlaget Bergen-Oslo-Tromsö, 1979
30 Christov R et al. Phys. Rev. Lett., 2006, **97**: 162001